

The stability of late-type stars close to the Eddington limit

Martin Asplund^{1,*}

Astronomiska observatoriet, Box 515, S-751 20 Uppsala, Sweden

Received 7 May 1997 / Accepted 10 September 1997

Abstract. The opacity-modified Eddington limit has been computed for hydrogen-deficient model atmospheres. The R Coronae Borealis (RCrB) stars are found to be located strikingly close to the limit, which suggests that the unknown trigger mechanism for their visual declines of the stars are instabilities in connection with the stars encountering the Eddington limit in their evolution. It also points to a similarity between the eruptive behaviours of the RCrB stars and the Luminous Blue Variables (LBVs).

Super-Eddington luminosities in hydrostatic model atmospheres manifest themselves by the presence of gas pressure inversions. Such inversions are not an artifact of the assumption of hydrostatic equilibrium but can also be present in hydrodynamical model atmospheres. Only for very large mass loss rates hardly realized in supergiants will the inversions be removed. Instabilities may, however, still be present in such inversions, which is investigated for both H-rich and H-deficient late-type supergiant model atmospheres. Dynamical instabilities may occur in surface ionization zones, which might lead to ejections of gas. A local, non-adiabatic, linear stability analysis reveals that sound waves can be amplified due to the strong radiative forces. However, despite the super-Eddington luminosities, the efficiency of the radiative instabilities is fairly low compared to for early-type stars with growth rates of 10^{-5} s^{-1} .

Key words: stars: model atmospheres – instabilities – stars: AGB and post-AGB – stars: mass-loss – stars: evolution – stars: variables: R Coronae Borealis – stars: variables: Luminous Blue Variables

1. The Eddington limit and the development of gas pressure inversions

The Eddington limit corresponds to a situation where the radiative acceleration outwards equals the gravitational acceleration inwards. Eddington (1926) originally only considered electron

scattering for the opacity (the classical Eddington limit), but in an ionization zone of an important element the true opacity can be much higher. Therefore, the opacity-modified Eddington limit in stellar atmospheres can occur at significantly greater gravities than the classical Eddington limit, as is evident for example from the calculations of Lamers & Fitzpatrick (1988), Gustafsson & Plez (1992) and Asplund & Gustafsson (1996).

If hydrostatic equilibrium is required, a stellar luminosity which locally exceeds the Eddington luminosity automatically forces the development of a gas pressure (P_{gas}) inversion, as seen from the equation of hydrostatic equilibrium:

$$\frac{dP_{\text{tot}}}{dr} = \frac{dP_{\text{gas}}}{dr} + \frac{dP_{\text{rad}}}{dr} = -g\rho. \quad (1)$$

From rearranging the above expression one obtains

$$\frac{1}{\rho} \frac{dP_{\text{gas}}}{dr} = -g_{\text{eff}} = -g(1 - g_{\text{rad}}/g) = -g[1 - \Gamma(r)], \quad (2)$$

with the radiative acceleration defined by:

$$g_{\text{rad}} = -\frac{1}{\rho} \frac{dP_{\text{rad}}}{dr} = \frac{1}{c} \int_0^{+\infty} \kappa_{\nu} F_{\nu} d\nu \quad (3)$$

(e.g. Mihalas 1978). Here F_{ν} denotes the physical flux and κ_{ν} the total mass extinction coefficient (with dimension $\text{cm}^2 \text{ g}^{-1}$). Obviously a positive P_{gas} -gradient must occur when the Eddington limit is encountered if hydrostatic equilibrium is valid.

It should be emphasized that a density inversion does not necessarily imply that the Eddington limit is exceeded. A density inversion predominantly occurs due to a changing molecular weight in the ionization zone of a dominant species, while a P_{gas} -inversion reflects a super-Eddington luminosity due to high opacity (Asplund et al. 1997a). Since both are related to ionization they may often occur in the same atmospheric layers, which has probably caused the confusion found in the literature (e.g. Maeder 1989).

It should be noted that P_{gas} -inversions only seem possible to develop in optically thick conditions. If the radiative acceleration exceeds gravity when lines dominate the opacity, the radiative force is highly unstable to perturbations induced by velocity gradients, since the spectral lines may then absorb unattenuated continuum flux. Therefore, rather than the development of a

Send offprint requests to: martin@nordita.dk

* Present address: NORDITA, Blegdamsvej 17, DK-2100 Copenhagen Ø, Denmark

P_{gas} -inversion, a stellar wind will be initiated, which is the case for radiatively driven winds of hot stars. The aim of the present study is to investigate whether P_{gas} -inversions in late-type stars, where the opacity instead is dominated by continuous opacity, are subject to a similar instability which would prevent their existence. Before considering possible instabilities, in Sect. 2 the derived Eddington limit for H-deficient stars is presented and a possible connection between the limit and the declines of the R Coronae Borealis (R CrB) stars is discussed.

2. The Eddington limit and the R CrB stars

2.1. The Eddington limit in the $T_{\text{eff}}\text{-log } g$ diagram

The location of the Eddington limit in a $T_{\text{eff}}\text{-log } g$ diagram can be estimated by model atmosphere calculations (Lamers & Fitzpatrick 1988; Gustafsson & Plez 1992). It should be emphasized that these models consistently include the radiative acceleration in the equation of hydrostatic equilibrium. Therefore, the location of the limit is not obtained by extrapolation towards lower gravities nor does it imply zero density, as has sometimes been claimed in the literature (e.g. Humphreys & Davidson 1994; Nieuwenhuijzen & de Jager 1995). An interesting conclusion from the above studies is that the theoretical opacity-modified Eddington limit coincides with the upper luminosity limit for stars (Lamers & Fitzpatrick 1988). It is therefore possible that the Eddington limit, possibly in connection with rotation (Langer 1997a,b; Owocki & Gayley 1997), prevents the evolution of stars into the super-Eddington regime by the existence of radiative instabilities. These may give rise to the eruptions of the Luminous Blue Variables (LBVs) (cf. Humphreys & Davidson 1994).

Here a similar investigation but for the H-deficient R CrB and related stars will be carried out; a preliminary report can be found in Asplund & Gustafsson (1996). The presence of P_{gas} -inversions in such model atmospheres was noted by Asplund et al. (1997a), who speculated that it may be the trigger mechanism for the enigmatic visual declines of the R CrB stars. The variability of these stars is likely due to the formation of an obscuring dust cloud close to the stellar surface in the line-of-sight, but how the dust condensation can proceed despite the relatively high equilibrium temperatures has long been an enigma (cf. Clayton 1996). The presence of shocks seems to be a very promising mechanism for the gas to cool sufficiently and thereby trigger dust formation (Woitke et al. 1996).

The models used here are recently constructed line-blanketed model photospheres with typical abundances of R CrB stars (Asplund et al. 1997a). In Fig. 1 the variation of Γ with optical depth is displayed for a sequence of models corresponding to constant luminosity and mass (e.g. $L_* = 8 \cdot 10^3 L_{\odot}$ and $M_* = 0.8 M_{\odot}$). The super-Eddington luminosities only occur in the deep atmospheric layers where He I ionizes and, as expected, where P_{gas} -inversions occur. Since the R CrB stars presumably evolve towards higher T_{eff} (Kilkenny 1982), the stars will move from the sub-Eddington regime into having super-Eddington luminosities, as is seen in Fig. 2 where the

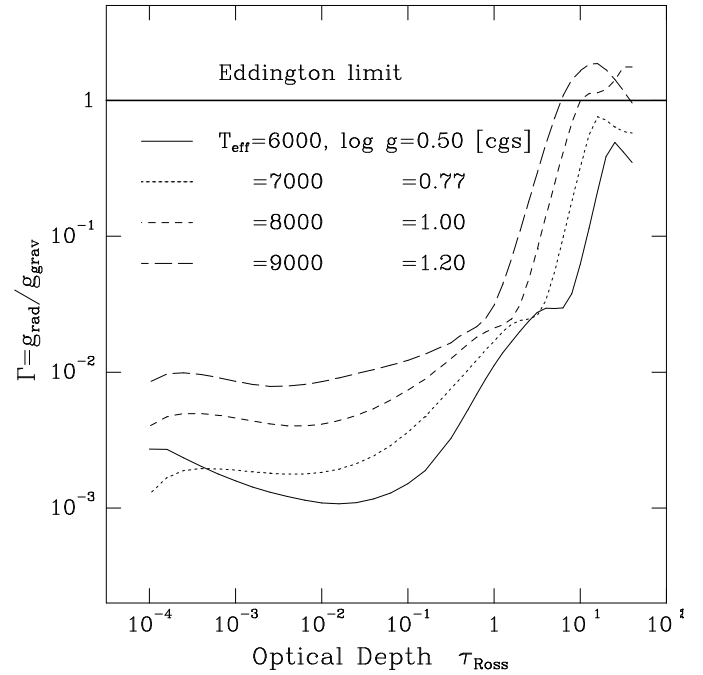


Fig. 1. Γ as a function of optical depth for a sequence of models with R CrB abundances at constant luminosity and mass. All models have $C/He = 1\%$. The $T_{\text{eff}} = 8000$ K model is only partly affected by convection in the inner layers, while the hottest model is not at all. Increased molecular absorption causes the slight increase in Γ towards the surface for the coolest model

theoretical Eddington limit in the $T_{\text{eff}}\text{-log } g$ diagram is shown. Compared with solar abundances the limit is shifted towards higher T_{eff} due to the higher ionization potential of He compared with H, but also extends to slightly larger $\log g$. The location of the Eddington limit for higher T_{eff} has not yet been explored, since a self-consistent hydrodynamical treatment is needed for $T_{\text{eff}} \gtrsim 13000$ K when $\Gamma > 1$ occurs for $\tau_{\text{Ross}} < 1$ and line opacity may determine g_{rad} .

The exact location of the computed Eddington limit will naturally depend on the detailed properties of the model atmospheres. For $T_{\text{eff}} \lesssim 8500$ K convection in the deeper layers of the He I ionization zone restricts the limit to lower $\log g$, since the radiative flux diminishes in the presence of a significant convective flux. Also, the lower temperatures decrease κ_{ν} and g_{rad} further. Including turbulent pressure would therefore bring the limit towards greater gravities by typically 0.2 dex, due to less efficient convection with lower densities. A C/He ratio of 1% has been assumed on the basis of the measured ratio in extreme helium (EHe) stars (Jeffery 1996), which presumably the R CrB stars are related to (Lambert et al. 1997). A higher carbon abundance pushes the Eddington limit towards higher gravities the same way as turbulent pressure does. A lower overall metallicity by 0.5 dex would decrease the limit by about 0.2 dex by lowering the temperatures in the inner layers with a diminished line-blanketing.

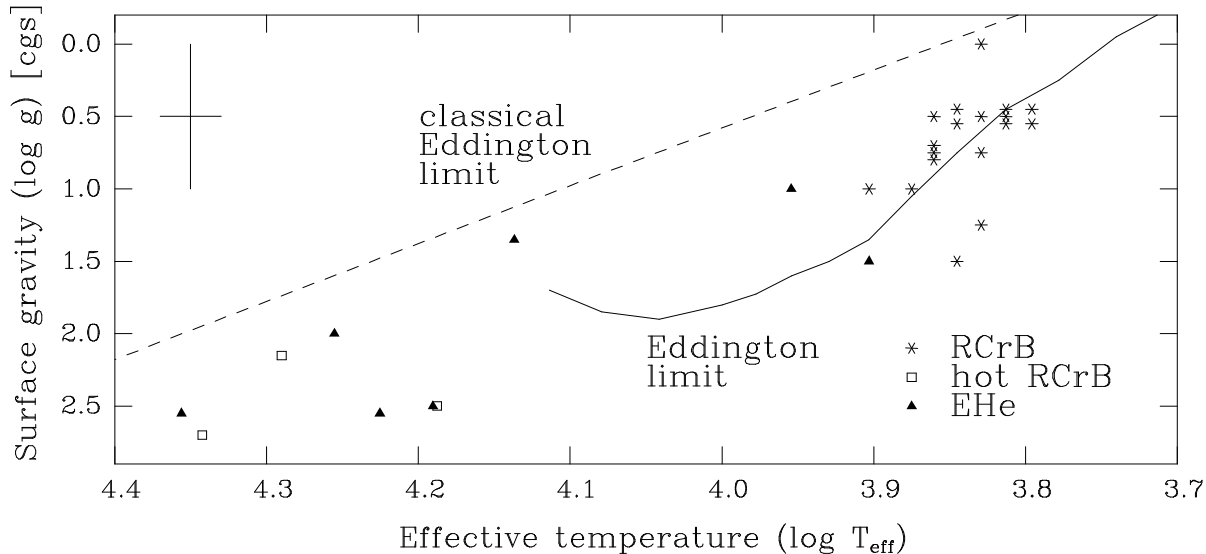


Fig. 2. The location of the opacity-modified Eddington limit (solid) in relation to the observed values of RCrB stars (Lambert et al. 1997; Asplund et al. 1997c). Also shown is the classical Eddington limit (dashed) and the hot RCrB and EHe stars with determined parameters (Jeffery 1996). The cross in the upper left corner illustrates the typical uncertainties in the estimated parameters of the RCrB stars

2.2. Possible consequences for H-deficient stars

In Fig. 2 the estimated parameters of the RCrB stars (Lambert et al. 1997; Asplund et al. 1997c) are also shown. Obviously, rather than being randomly located in the diagram as one a priori might have guessed, the RCrB stars fall close to the limit, which suggests that a connection between the declines of RCrB stars and the Eddington limit exists. Thus, there is an alluring resemblance between the RCrB stars and the Luminous Blue Variables in their proximity to the Eddington limits and their eruptive behaviours (Asplund & Gustafsson 1996). If the RCrB stars are evolving towards higher T_{eff} (Kilkenny 1982) and the EHe domain at constant luminosity, their immediate progenitors should be the H-deficient carbon (HdC) stars (Lambert et al. 1997). The EHe and HdC stars experience no visual fadings despite being otherwise similar to the RCrB stars. It is therefore plausible that the reason for the non-variability is that the HdC stars have not yet reached the Eddington limit while the EHe stars are located on the stable side of the limit at higher T_{eff} .

If the declines of the RCrB stars are indeed triggered by the super-Eddington luminosities, one could expect a correspondence between the maximum value of Γ in the atmosphere and frequency of declines. In the pulsation-induced dust condensation model for the RCrB stars (Woitke et al. 1996), in which the dust formation is triggered by propagating shock waves due to ordinary pulsations, one would sooner expect a correlation with pulsation strength. Intriguingly, V854 Cen, which is the RCrB star most frequent in decline, has very weak photospheric pulsations (Lawson & Cottrell 1997) but by a wide margin the largest Γ found of the 18 RCrB stars analysed sofar. RY Sgr, on the other hand, has by far the strongest photospheric pulsations but only average amount of declines, which might reflect the fact that Γ is not unusually high. Pulsation may, however,

push some stars across the limit by periodically shifting them towards higher T_{eff} , e.g. $\Delta T_{\text{eff}} = \pm 250$ K for RCrB itself (Rao & Lambert 1997).

The proposed connection between the Eddington limit and the declines of the RCrB stars is certainly not without problems, which deserve to be addressed further. A few stars seem not to behave as expected if the proposal is correct. In particular this is true for some of the coolest EHe stars and the three hot RCrB stars.

3. The disappearance of gas pressure inversions

3.1. Effects of convection

As seen above, a P_{gas} -inversion must develop at the Eddington limit in hydrostatic equilibrium. One should ask, however, whether strong convection may take place to prevent it, since the ionization zone causing the high opacity and thereby the super-Eddington luminosities also favours convection. In fact, a super-Eddington luminosity in the diffusion regime automatically requires the presence of convection as shown by Langer (1997a). Generalizing Langer's derivation for a non-negligible radiation pressure to also include the effects of ionization, the Schwarzschild criterion $\nabla_{\text{rad}} > \nabla_{\text{ad}}$ for the onset of convection is equivalent to

$$\Gamma(r) > \frac{4\alpha \{2 + 8\alpha + x(1-x) [5/2 + \epsilon/kT + 4\alpha]\}}{5 + 40\alpha + 32\alpha^2 + x(1-x) [5/2 + \epsilon/kT + 4\alpha]^2} \quad (4)$$

(e.g. Mihalas & Weibel Mihalas 1984). Here $\alpha = P_{\text{rad}}/P_{\text{gas}}$, while x denotes the ionization fraction of the most abundant element with an ionization potential ϵ . Convection must be initiated as $\Gamma(r)$ approaches unity, since the right hand side is always less than 1. Thereby the radiative flux and hence Γ diminishes when

convection is efficient. The Eddington limit can therefore not be exceeded in adiabatic convection zones in the stellar interior and hence P_{gas} -inversions will not develop. Thus, inversions can only be present in non-adiabatic convection zones close to the stellar surface.

It should be remembered that the location of the Eddington limit is dependent on the convection treatment. A P_{gas} -inversion will for example disappear if the density scale height is applied instead of the normal pressure scale height for the calculation of the convective flux through the mixing length theory. The mixing length theory is rarely a good description of stellar convection, and in particular for these extreme situations it may be very misleading. Ultimately, hydrodynamical simulations will be necessary to investigate the effects of convection on P_{gas} -inversions.

3.2. Effects of mass loss

Using the momentum equation one can investigate under which conditions a P_{gas} -inversion can exist in the presence of a stellar mass loss. Or equivalently: which mass loss rates can one expect from a star if the super-Eddington luminosities would instead drive a stellar wind?

In the presence of a stellar outflow, the equation of hydrostatic equilibrium must be replaced with the momentum equation:

$$v \frac{dv}{dr} = -\frac{1}{\rho} \frac{dP_{\text{gas}}}{dr} - g_{\text{eff}}, \quad (5)$$

where we have restricted ourselves to the one-dimensional, time-independent case. Also other external forces, such as turbulent forces ($g_{\text{turb}} = -1/\rho \cdot dP_{\text{turb}}/dr$) and centrifugal forces ($g_{\text{cent}} = v_{\text{rot}}^2(r, \theta)/r$), can be contained in g_{eff} besides radiation. It should therefore be kept in mind that the possibility of an instability may be underestimated when restricting the following discussion to only radiative forces, as other forces also tend to be destabilizing (e.g. Nieuwenhuijzen & de Jager 1995; Langer 1997a,b; Owocki & Gayley 1997).

Together with a constant, spherically symmetric mass loss rate $\dot{M} = 4\pi r^2 \rho v$, and the equation of state $P_{\text{gas}} = \mathcal{R} \rho T / \mu$, it is possible to rewrite the momentum equation into the so called “wind equation”:

$$(v^2 - c_{\text{T}}^2) \frac{1}{v} \frac{dv}{dr} = c_{\text{T}}^2 \left(\frac{2}{r} - \frac{1}{T} \frac{dT}{dr} + \frac{1}{\mu} \frac{d\mu}{dr} \right) - g_{\text{eff}}, \quad (6)$$

where the isothermal sound speed defined by $c_{\text{T}}^2 = (\partial P_{\text{gas}} / \partial \rho)_{\text{T}} = P_{\text{gas}} / \rho$ has been introduced. By an inspection of Eq. 6, it is possible to determine under which circumstances ρ - or P_{gas} -inversions are allowed. In normal cases, $d\mu/dr \geq 0$ in the surface layers and therefore the parenthesis on the right hand side of Eq. 6 is positive as long as a temperature inversion is not present, which is not possible in optically thick layers with a radiative flux. Therefore, if $g_{\text{rad}} > g$ but $v < c_{\text{T}}$, the velocity gradient dv/dr must be negative. Since a constant \dot{M} has been assumed, a density inversion will be present if $r/v \cdot dv/dr + 2 < 0$

and therefore a P_{gas} -inversion is possible (though not required). If, on the other hand, $v > c_{\text{T}}$ while $g_{\text{rad}} > g$, then dv/dr must be positive, and the density gradient cannot be positive: a density inversion cannot exist. Since a P_{gas} -inversion requires a density inversion, neither inversion can occur in the stellar atmosphere despite the super-Eddington luminosities. Again the possibility of a temperature inversion has been neglected. A sufficient criterion for the disappearance of a P_{gas} -inversion is therefore that the outflow velocity due to mass loss is high enough ($v \geq c_{\text{T}}$).

The critical mass loss rate can be estimated by comparing $v = \dot{M}/4\pi r^2 \rho$ with c_{T} . The values for c_{T} and ρ will be taken from static models, which is justified for these rough estimates, since the atmosphere below the sonic point is normally little affected by mass loss. A model atmosphere with $T_{\text{eff}} = 7000$ K, $\log g = 0.5$ [cgs] and solar abundances requires a critical mass loss rate $\dot{M}_{\text{crit}} \approx 6 \cdot 10^{-4} (M_*/M_{\odot}) M_{\odot} \text{ yr}^{-1}$. Hence P_{gas} -inversions can exist in stars despite high mass loss rates. Achmad & Lamers (1997) have arrived at similar conclusions and estimates. They also verify the finding numerically with dynamical steady state atmospheres, though not altogether self-consistently.

An even higher critical mass loss rate is found for the R CrB stars. The lack of hydrogen makes the continuous opacity significantly lower than for solar abundances and hence the density at a given optical depth will be correspondingly greater, typically by a factor of 50 (Asplund et al. 1997a). Since the density is higher, the outflow velocity will be lower in order to carry the same \dot{M} . A similar model as above but with abundances typical for R CrB stars, will therefore require $\dot{M}_{\text{crit}} \approx 3 \cdot 10^{-2} (M_*/M_{\odot}) M_{\odot} \text{ yr}^{-1}$. The mass loss rates of R CrB stars are poorly known, in particular since it may be episodic, but rough estimates suggest $\dot{M} \sim 10^{-6} M_{\odot} \text{ yr}^{-1}$ (e.g. Feast 1986), orders of magnitude smaller than \dot{M}_{crit} .

It is concluded that P_{gas} -inversions are not an artifact of hydrostatic equilibrium but may also exist in dynamical steady state atmospheres, even with a high mass loss rate.

4. Dynamical instabilities

Dynamical stability has been extensively studied, in particular in connection with the termination of the AGB (e.g. Paczyński & Ziółkowski 1968; Wagenhuber & Weiss 1994). Radial adiabatic oscillations will grow exponentially in time for dynamical instability, which is formally encountered if the first generalized adiabatic exponent

$$\Gamma_1 = \left(\frac{\partial \ln P_{\text{tot}}}{\partial \ln \rho} \right)_{\text{ad}} \quad (7)$$

is less than 4/3 in a region effectively isolated from the rest of the star. An ideal gas has $\Gamma_1 = 5/3$ while pure radiation has $\Gamma_1 = 4/3$, but the combined effect of non-negligible radiation pressure and ionization may push Γ_1 below the limiting value. For dynamical instability to occur, the pressure weighted vol-

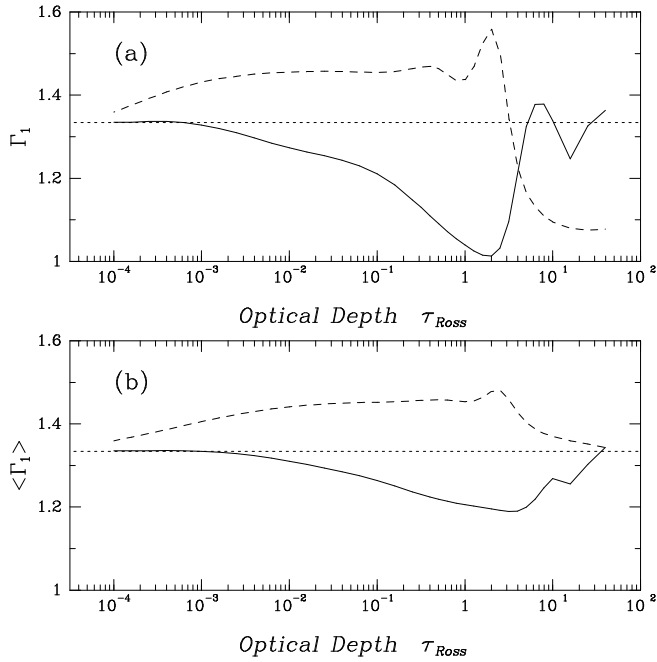


Fig. 3. **a** The generalized first adiabatic exponent Γ_1 as a function of optical depth in model atmospheres with solar (solid) and R CrB (dashed) compositions. **b** The pressure weighted first adiabatic exponent $\langle \Gamma_1 \rangle$ for the same models as in **a**. In both panels the parameters are $T_{\text{eff}} = 7000$ and $\log g = 0.50$. Values below the dotted lines at $\Gamma_1 = \langle \Gamma_1 \rangle = 4/3$ correspond formally to dynamical instability

umetric mean value of Γ_1 between the depth r and the stellar surface R_*

$$\langle \Gamma_1 \rangle = \frac{\int_r^{R_*} \Gamma_1 P_{\text{tot}} dV}{\int_r^{R_*} P_{\text{tot}} dV} \quad (8)$$

must be reduced below $4/3$ in a significant fraction of the star. Stars with a pronounced core-envelope structure and high luminosity-to-mass ratios, like the supergiants investigated here, may show dynamical instabilities in ionization zones (e.g. Stothers & Chin 1993; Wagenhuber & Weiss 1994).

In Fig. 3 the run of Γ_1 and $\langle \Gamma_1 \rangle$ as functions of optical depth are shown for two model atmospheres corresponding to $T_{\text{eff}} = 7000$ and $\log g = 0.50$ for a solar and a H-deficient composition. In particular, $\langle \Gamma_1 \rangle$ is reduced much below $4/3$ for the model with solar abundances in the H I and He I ionization zones. At the surface P_{rad} dominates the total pressure and hence Γ_1 is very close to $4/3$. A more complete study for H-rich model atmospheres has been presented by Lobel et al. (1992), who arrive at the same conclusions. In the R CrB model only the He I ionization zone exists, which explains the quite different depth variation of Γ_1 . The higher temperatures at depth in the H-deficient model make He I ionization occur at smaller τ_{Ross} . Also seen is the minor effect of the C I ionization zone at $\tau_{\text{Ross}} \simeq 1$. These models only extend down to $\tau_{\text{Ross}} = 40$ and hence it is not possible to tell how $\langle \Gamma_1 \rangle$ varies further in, though the He II ionization zone will also reduce Γ_1 .

It seems that atmospheres of late-type supergiants are close to being dynamically unstable, or may even be so for sufficiently high luminosity-to-mass ratios. Violent instabilities due to this might lead to ejection of material, as found for the termination of the AGB (Wagenhuber & Weiss 1994), as well as for the LBVs (Stothers & Chin 1993). Also R CrB stellar models seem to suffer from a similar dynamical instability as the stars on the tip of the AGB (A. Weiss, private communication). It should be remembered though that the above-mentioned evolutionary studies lack a proper hydrodynamical treatment, and therefore interpreting the instabilities found in the models as actually occurring in the stars must still be made with some caution.

5. Radiative instabilities

5.1. Radiatively driven sound waves in P_{gas} -inversions

It is clear from the discussion in Sect. 3 and 4 that P_{gas} -inversions may exist in stars with high luminosity-to-mass ratios and that such stars are close to being dynamically unstable. Thus, these stars may be vulnerable to radiative instabilities, since the additional destabilization from radiative forces may render them unstable.

The existence of radiatively driven sound waves in hot stars due to high g_{rad} has been suggested by Hearn (1972, 1973), and further elaborated by Berthomieu et al. (1976), Spiegel (1976) and Carlberg (1980). The instability is based on the increase in opacity upon compression, since the radiation force is in phase with the velocity perturbation and hence causes amplification. For these high temperatures it requires essentially isothermal perturbations, since

$$(\partial \kappa_{\text{F}} / \partial \rho)_{\text{T}} + (\Gamma_3 - 1)(\partial \kappa_{\text{F}} / \partial T)_{\rho} < 0. \quad (9)$$

Here $\Gamma_3 - 1 = (\partial \ln T / \partial \ln \rho)_{\text{ad}}$, while κ_{F} is the flux weighted mean opacity. Thus only short wavenumbers will be amplified. The growth rate is especially high as Γ approaches unity (Berthomieu et al. 1976) but the super-Eddington case has not been investigated. Carlberg (1980) found that the instability may provide rapid transfer of momentum from the radiation to the gas with typical growth rates of 10^{-3} s^{-1} for $T_{\text{eff}} \sim 50000 \text{ K}$. It is possible that a similar instability is exhibited also in late-type supergiants, with the important differences being the super-Eddington luminosities in the P_{gas} -inversions and that isothermal perturbations are not necessary, since both $(\partial \kappa_{\text{F}} / \partial \rho)_{\text{T}} > 0$ and $(\partial \kappa_{\text{F}} / \partial T)_{\rho} > 0$ in the upper layers of the P_{gas} -inversions (Fig. 4).

To study the stability of a P_{gas} -inversion a local, linear, non-adiabatic stability analysis has been carried out. Small, sinusoidal perturbations around the equilibrium values are assumed for the temperature, density and vertical velocity:

$$\begin{aligned} T &= T_0 + T_1 \cdot e^{i(kr - \omega t)} \\ \rho &= \rho_0 + \rho_1 \cdot e^{i(kr - \omega t)} \\ v &= v_0 + v_1 \cdot e^{i(kr - \omega t)}, \end{aligned}$$

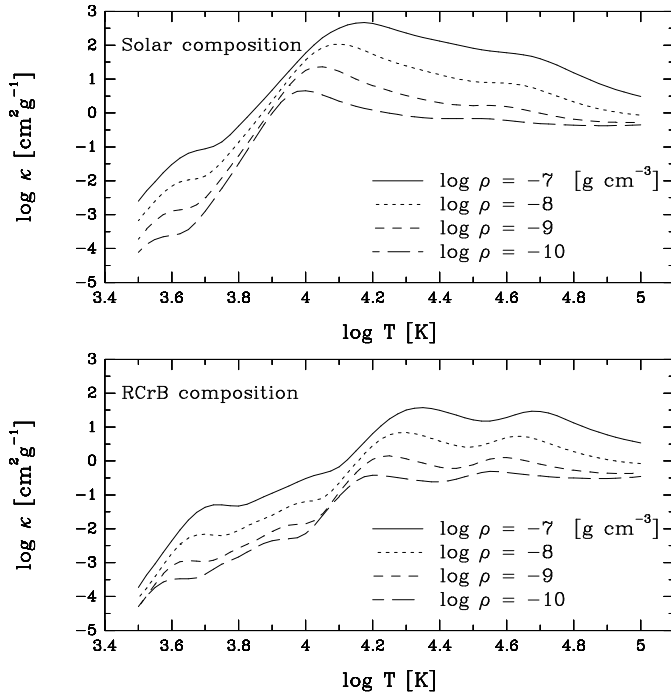


Fig. 4. The dependence of the Rosseland mean opacity on temperature and density for **a** solar abundances and **b** R CrB abundances. The atomic data for the opacities are taken from the Opacity Project (Seaton et al. 1994 and references therein). The top of the P_{gas} -inversion for a model atmosphere with $T_{\text{eff}} = 7000$ K and $\log g = 0.5$ occurs at $\log T \approx 3.9$ for solar abundances and at $\log T \approx 4.1$ for an R CrB composition

where T_1, ρ_1 and v_1 are small. The atmosphere is assumed to be static ($v_0 = 0$), since the outflow velocity must anyway be less than the isothermal sound speed for a P_{gas} -inversion to exist, as demonstrated above. The analysis will be restricted to vertical motion and therefore multi-dimensional instabilities of Rayleigh-Taylor-type will not be found. Carlberg (1980) investigated also such a gradient instability for hot stars but found slow growth rates compared to the radiatively driven sound waves. Such a gradient instability would resemble convective motion which, however, is already present in the layers of interest in the unperturbed model and is thus not specifically searched for here.

The equations to be linearized are the material equations for conservation of mass, momentum and energy:

$$\frac{D\rho}{Dt} + \rho(\nabla \cdot \mathbf{v}) = 0 \quad (10)$$

$$\frac{D\mathbf{v}}{Dt} + \frac{1}{\rho}\nabla P_{\text{gas}} = -g_{\text{eff}}\hat{\mathbf{r}} \quad (11)$$

$$\rho \frac{De}{Dt} - \frac{P_{\text{gas}}}{\rho} \frac{D\rho}{Dt} = 4\pi\rho\kappa_{\text{Ross}}^{\text{abs}}(J - B) - \rho\mathbf{v} \cdot g_{\text{rad}}\hat{\mathbf{r}} \quad (12)$$

(e.g. Mihalas & Weibel Mihalas 1984), where D/Dt , e , B and J denote the Lagrangean co-moving derivative, the specific internal energy of the gas, the wavelength integrated Planck function ($B = \int_0^\infty B_\nu(T)d\nu$) and mean intensity ($J = \int_0^\infty J_\nu d\nu$), respectively. The absorption and Planck mean opacities have

been replaced by the Rosseland mean opacity for absorption $\kappa_{\text{Ross}}^{\text{abs}} = \kappa_{\text{Ross}} - \sigma$, which is a good approximation for the relevant optical depths. The scattering contribution to the total extinction is here denoted by σ . Furthermore LTE ($S_\nu = B_\nu$) has been assumed.

The material equations must be coupled to the equations for the radiation field to account for radiative transfer effects through exchanges of energy and momentum between the photons and the gas. In this exploratory investigation the effects of radiation are included with a time-independent treatment, i.e. the radiation field is assumed to be quasi-static. The radiation momentum and energy equations will then look like:

$$\frac{dK}{dr} = -\rho\kappa_{\text{F}}H \quad (13)$$

$$\frac{dH}{dr} = \rho(\kappa_{\text{Ross}} - \sigma)(B - J). \quad (14)$$

Here H and K denote the wavelength integrated Eddington flux ($H = (1/4\pi)\int_0^\infty F_\nu d\nu$) and radiation pressure ($K = (c/4\pi)P_{\text{rad}}$) respectively. In the diffusion regime for the unperturbed atmosphere, $\kappa_{\text{F}} = \kappa_{\text{Ross}}$ is valid. The equilibrium radiation quantities are related by:

$$J_0 = B_0 = 4(T_0/T_{\text{eff}})^4 H_0 = \sigma_{\text{R}}T_0^4/\pi. \quad (15)$$

For the first relation radiative equilibrium is implicitly imposed, which is not strictly true in the cases which will be investigated below. However, the analysis will be restricted only to atmospheric depths where the convective flux carries $< 10\%$ of the total flux (i.e. in the upper part of the convection zone) and radiative equilibrium can therefore be largely justified. To close the relations the Eddington approximation ($K = J/3$) will be made, which is, like LTE, well justified in the atmospheric layers of interest. In the following, the radiation energy and momentum equations will be combined to a single equation, which means that there is one more variable to perturb, for which J is chosen:

$$J = J_0 + J_1 \cdot e^{i(kr - \omega t)}.$$

Together with the definitions of the isothermal sound speed c_{T} , the density scale height $H_\rho = -[d\ln\rho/dr]^{-1}$ and an ideal gas for P_{gas} , linearization to first order yields:

$$\begin{aligned} \frac{\rho_1}{\rho_0}[-i\omega] + v_1[ik - H_\rho^{-1}] &= 0 \quad (16) \\ \frac{\rho_1}{\rho_0} \left[g + c_{\text{T}}^2 \left(ik + \frac{1}{T_0} \frac{dT}{dr} - \frac{1}{\mu_0} \frac{d\mu}{dr} \right) \right] &+ \\ + \frac{\rho_1}{\rho_0} \left[-c_{\text{T}}^2 \mu_\rho \left(ik - H_\rho^{-1} + \frac{1}{T_0} \frac{dT}{dr} - \frac{2}{\mu_0} \frac{d\mu}{dr} \right) \right] &+ \\ + \frac{T_1}{T_0} \left[c_{\text{T}}^2 \left(ik - H_\rho^{-1} - \frac{1}{\mu_0} \frac{d\mu}{dr} \right) \right] &+ \\ + \frac{T_1}{T_0} \left[-c_{\text{T}}^2 \mu_T \left(ik - H_\rho^{-1} + \frac{1}{T_0} \frac{dT}{dr} - \frac{2}{\mu_0} \frac{d\mu}{dr} \right) \right] &+ \\ + v_1[-i\omega] + \frac{J_1}{J_0} \left[-ik \frac{4\sigma_{\text{R}}T_0^4}{3c\rho_0} \right] &= 0 \quad (17) \end{aligned}$$

Table 1. Local values of the atmospheric structure. Both the model with a solar and an R CrB composition have $T_{\text{eff}} = 7000$ and $\log g = 0.5$

| Variable | Units | Solar | R CrB |
|---|-------------------------------|------------------------|------------------------|
| $\log \tau_{\text{Ross}}$ | | 0.5 | 1.2 |
| g_{rad} | $[\text{cm s}^{-2}]$ | $1.29 \cdot 10^1$ | $4.31 \cdot 10^0$ |
| T | [K] | 9610 | 14950 |
| ρ | $[\text{g cm}^{-3}]$ | $4.62 \cdot 10^{-11}$ | $4.96 \cdot 10^{-9}$ |
| P_{gas} | $[\text{dyn cm}^{-2}]$ | $5.19 \cdot 10^1$ | $1.92 \cdot 10^3$ |
| c_s | $[\text{cm s}^{-1}]$ | $1.32 \cdot 10^6$ | $6.67 \cdot 10^5$ |
| $(1/T)dT/dr$ | $[\text{cm}^{-1}]$ | $-6.67 \cdot 10^{-12}$ | $-3.15 \cdot 10^{-11}$ |
| $(1/\rho)d\rho/dr$ | $[\text{cm}^{-1}]$ | $2.10 \cdot 10^{-11}$ | $9.87 \cdot 10^{-11}$ |
| $(1/\mu)d\mu/dr$ | $[\text{cm}^{-1}]$ | $5.92 \cdot 10^{-12}$ | $6.50 \cdot 10^{-11}$ |
| κ_{Ross} | $[\text{cm}^2 \text{g}^{-1}]$ | $2.50 \cdot 10^0$ | $9.11 \cdot 10^{-1}$ |
| σ | $[\text{cm}^2 \text{g}^{-1}]$ | $2.55 \cdot 10^{-1}$ | $2.94 \cdot 10^{-2}$ |
| $\partial \ln \kappa / \partial \ln T$ | | $2.43 \cdot 10^{-1}$ | $1.32 \cdot 10^1$ |
| $\partial \ln \kappa / \partial \ln \rho$ | | $6.75 \cdot 10^{-1}$ | $1.72 \cdot 10^{-1}$ |
| de/dr | $[\text{cm}^1 \text{s}^{-2}]$ | $-1.29 \cdot 10^2$ | $-5.15 \cdot 10^2$ |
| $\rho(\partial e / \partial \rho)_T$ | $[\text{cm}^2 \text{s}^{-2}]$ | $-2.15 \cdot 10^{12}$ | $-8.21 \cdot 10^{11}$ |
| $T(\partial e / \partial T)_\rho$ | $[\text{cm}^2 \text{s}^{-2}]$ | $2.14 \cdot 10^{13}$ | $1.63 \cdot 10^{13}$ |

second the same but for an R CrB star. As before, both model atmospheres have $T_{\text{eff}} = 7000$ K and $\log g = 0.5$. Values for some of the physical parameters at some atmospheric layer where the instability may occur are found in Table 1.

The calculated growth rates are shown in Fig. 5a and b, which reveals amplification for $k \lesssim 2 \cdot 10^{-8} \text{ cm}^{-1}$ (solar composition) and $k \lesssim 2 \cdot 10^{-7} \text{ cm}^{-1}$ (R CrB composition). For large k , the perturbations are as expected damped due to the negligible optical depths of the disturbances ($\tau_\Lambda = 2\pi\kappa\rho/k$), which make the sound waves little affected by the radiative forces. Instead, the smoothing effects from radiation energy exchange due to large gradients in the perturbed variables dominate. The maximum growth rates are slightly smaller for a solar composition than for a H-deficient composition: $1.3 \cdot 10^{-5}$ respectively $4.3 \cdot 10^{-5} \text{ s}^{-1}$, which corresponds to an e-folding time on the order of the sound crossing time of the atmosphere. For the largest wavenumbers with such growth rates, the real parts are significantly higher, which implies that the sound waves are only slightly amplified per wavelength. For smaller k , however, the growth rate is comparable with the oscillation rate. In fact, for the model with solar composition, the wave is essentially non-propagating for the smallest k . However, the use of a local analysis is not justified when the wavelengths of the perturbations are comparable with the scale heights of the variations for the variables. For $k \gtrsim 10^{-10} \text{ cm}^{-1}$, the propagation speed is slightly less than the isothermal sound speed in both cases.

Thus, radiation-modified sound waves can be amplified in late-type stars with significant radiative forces. However, the perturbations are not very strongly excited with minimum growth times $\simeq 10^5$ s, contrary to the findings by Carlberg (1980) for hot stars, mainly as a result of the much smaller radiative fluxes ($F \propto T_{\text{eff}}^4$). For the instability to generate large amplification, the sound waves must be reflected at the surface and pass through the region with high radiative forces several times. However, the inwards propagating modes are damped for the same reason as the outgoing are amplified, with the magnitude of the damping rate similar to the growth rate, which suggests that the instability will still not be very efficient. In order to estimate the behaviour of the instability in the global, non-linear regime, a more sophisticated study than presented here must be carried out.

$$\begin{aligned}
& \frac{\rho_1}{\rho_0} \left[-i\omega \left(\rho_0 \frac{\partial e}{\partial \rho} - c_T^2 \right) \right] + \\
& + \frac{T_1}{T_0} \left[-i\omega T_0 \frac{\partial e}{\partial T} + 16(\kappa_0 - \sigma_0) \sigma_R T_0^4 \right] + \\
& + v_1 \left[g_{\text{rad}} + \frac{de}{dr} + c_T^2 H_\rho^{-1} \right] + \\
& + \frac{J_1}{J_0} \left[-4(\kappa_0 - \sigma_0) \sigma_R T_0^4 \right] = 0 \quad (18)
\end{aligned}$$

$$\begin{aligned}
& \frac{\rho_1}{\rho_0} \left[-\frac{ik}{\rho_0(\kappa_0 - \sigma_0)} \frac{1}{4} \left(\frac{T_{\text{eff}}}{T_0} \right)^4 \left(1 + \frac{\partial \ln \kappa}{\partial \ln \rho} \right) \right] + \\
& + \frac{T_1}{T_0} \left[-4 - \frac{ik}{\rho_0(\kappa_0 - \sigma_0)} \frac{1}{4} \left(\frac{T_{\text{eff}}}{T_0} \right)^4 \frac{\partial \ln \kappa}{\partial \ln T} \right] + \\
& + \frac{J_1}{J_0} \left[1 + \frac{k^2}{3\kappa_0(\kappa_0 - \sigma_0)\rho_0^2} \right] = 0. \quad (19)
\end{aligned}$$

The notation has been abbreviated according to $\mu_\rho = (\rho_0/\mu_0)(\partial\mu/\partial\rho)$ and $\mu_T = (T_0/\mu_0)(\partial\mu/\partial T)$. Derivatives with respect to v and J have been ignored, which is justified in optically thick layers where line opacity is unimportant. True enough, photoionization edges introduce some velocity dependence on g_{rad} but this minor effect is neglected.

In order for the above set of equations to have a non-trivial solution for the perturbations T_1 , ρ_1 , v_1 and J_1 , the determinant of the equations must be equal to 0. The three complex eigenvalues w for a given real wavenumber k then correspond to the allowed perturbations. Two of the modes will represent radiation-modified gravity-acoustic waves while the third is a non-propagating, heavily damped, thermal wave. Here two different cases will be investigated numerically, one corresponding to a P_{gas} -inversion in a supergiant with solar abundances and the

5.2. The simplifying case of a isothermal, non-ionizing atmosphere

In order to gain further theoretical insight into which atmospheric properties contribute to the instability presented above, the equations can be simplified by assuming the unperturbed atmosphere to be isothermal and neglecting ionization and scattering. Furthermore, only the limits of optically thin and optically thick disturbances will be studied and hence the combined radiative energy and momentum equation will not be needed. The gas energy equation will thus instead be written as:

$$\rho \frac{De}{Dt} - \frac{P_{\text{gas}}}{\rho} \frac{D\rho}{Dt} = -\mathcal{L} \quad (20)$$

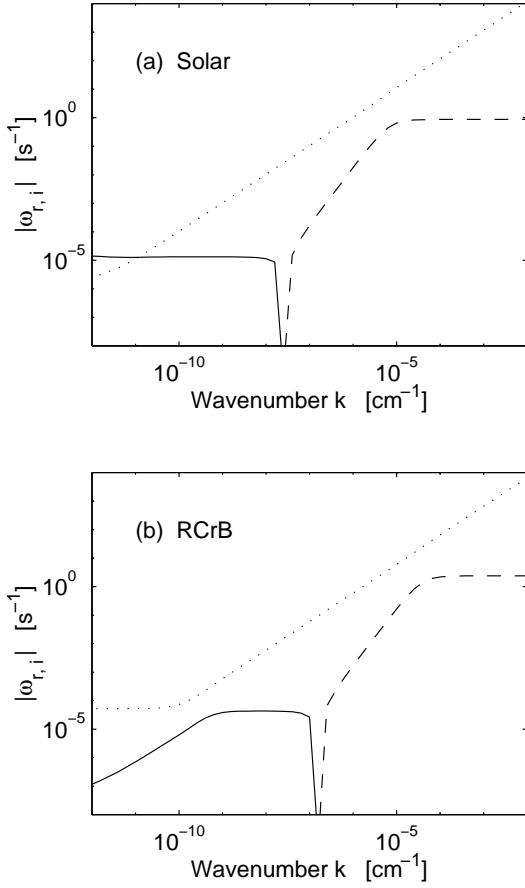


Fig. 5a and b. The numerical solutions to the full set of linearized equations for the gravity-acoustic wave modes for **a** solar and **b** RCrB compositions. The real parts are the dotted curves. The solid lines correspond to amplification of the imaginary parts, while the dashed curves represent damping. For wavenumbers with damping, the absolute magnitude of the imaginary part is shown

where \mathcal{L} denotes the net radiative cooling rate of the gas. Depending on the optical thickness of the disturbance, \mathcal{L} will be described by either Newtonian cooling or equilibrium diffusion (e.g. Mihalas & Weibel Mihalas 1984). The rate of work done by g_{rad} has been ignored.

The linearized continuity equation remains the same but the linearized momentum equation reads as:

$$\frac{\rho_1}{\rho_0} [c_T^2 ik + g_{\text{eff}} - g_\rho] + \frac{T_1}{T_0} [c_T^2 (ik - H_\rho^{-1}) - g_T] + v_1 [-i\omega] = 0, \quad (21)$$

where $g_\rho = \rho_0 \partial g_{\text{rad}} / \partial \rho$ and $g_T = T_0 \partial g_{\text{rad}} / \partial T$, while the energy equation looks like:

$$\frac{\rho_1}{\rho_0} [-i\omega] + \frac{T_1}{T_0} \left[\frac{i\omega}{\gamma - 1} - \mathcal{L} \right] + v_1 [-H_\rho^{-1}] = 0. \quad (22)$$

Here \mathcal{L} represents the term arising from the net cooling rate \mathcal{L} and γ the ratio of specific heats. For Newtonian cooling

$$\mathcal{L} = \frac{16\kappa_{\text{Ross}}\sigma_{\text{R}}T_0^4}{(\gamma - 1)c_{\text{v}}T} \quad (23)$$

and in the diffusion regime

$$\mathcal{L} = \frac{16\kappa_{\text{Ross}}\sigma_{\text{R}}T_0^4}{(\gamma - 1)c_{\text{v}}T} \cdot \frac{k^2}{3\kappa_{\text{Ross}}^2\rho^2}. \quad (24)$$

\mathcal{L} is the inverse of the radiative cooling time-scale (e.g. Mihalas & Weibel Mihalas 1984), where the factor $k^2/(3\kappa_{\text{Ross}}^2\rho^2) \ll 1$ takes into account the optical depth effects for optically thick conditions. The simplified dispersion relation then reads:

$$\begin{aligned} & -i\omega^3 + \omega^2 \mathcal{L} (\gamma - 1) + \\ & + i\omega [\gamma k^2 c_T^2 + H_\rho^{-1} (g_{\text{eff}} - g_\rho)] + \\ & - \omega k [g_\rho + (\gamma - 1)g_T - g_{\text{eff}} + \gamma c_T^2 H_\rho^{-1}] + \\ & - \mathcal{L} (\gamma - 1) [k^2 c_T^2 + H_\rho^{-1} (g_{\text{eff}} - g_\rho)] + \\ & - ik \mathcal{L} (\gamma - 1) [g_\rho - g_{\text{eff}} + c_T^2 H_\rho^{-1}] = 0. \end{aligned} \quad (25)$$

For $k \gtrsim 10^{-10} \text{ cm}^{-1}$, $H_\rho^{-1} (g_{\text{eff}} - g_\rho)$ is much smaller than $k^2 c_T^2$ for the two investigated models and can be ignored.

In situations of rapid radiative cooling ($\mathcal{L} \gg \omega$), the dispersion relation can be simplified to yield the solutions

$$\omega \simeq \pm \left[kc_T + \frac{i}{2c_T} \{g_\rho - g_{\text{eff}} + H_\rho^{-1} c_T^2\} \right], \quad (26)$$

i.e. isothermally propagating, radiation-modified sound waves. In the limit of slow cooling ($\mathcal{L} \ll \omega$), as expected adiabatic acoustic waves are recovered:

$$\omega \simeq \pm \left[kc_s + \frac{i}{2c_s} \{g_\rho + (\gamma - 1)g_T - g_{\text{eff}} + H_\rho^{-1} c_s^2\} \right], \quad (27)$$

which travel with the adiabatic sound speed $c_s = (\partial P_{\text{gas}} / \partial \rho)_s = \gamma P_{\text{gas}} / \rho$. For $k \lesssim 10^{-10} \text{ cm}^{-1}$, the propagation speed will be modified by the neglected terms $H_\rho^{-1} (g_{\text{eff}} - g_\rho)$, though the growth/damping rates will remain the same.

For both isothermal and adiabatic perturbations, the sound waves are amplified by the action of the radiative acceleration, as long as the opacity increases with temperature and density (assuming constant radiative flux):

$$g_\rho = \frac{\sigma T_{\text{eff}}^4}{c} \cdot \rho \frac{\partial \kappa_{\text{F}}}{\partial \rho} \quad (28)$$

$$g_T = \frac{\sigma T_{\text{eff}}^4}{c} \cdot T \frac{\partial \kappa_{\text{F}}}{\partial T}. \quad (29)$$

Furthermore, in a P_{gas} -inversion g_{eff} is negative and hence tends to excite an initial disturbance. However, the normal momentum conservation counteracts this due to propagation in a density stratified medium; the density inversion will tend to damp the amplitude for outwards propagating waves. In fact, with this simplified atmosphere and the values in Table 1, in both models

the last term dominates. Hence, the amplitude of sound waves will decay as they propagate outwards with these assumptions, despite the super-Eddington luminosities and the increase in opacity upon compression. Thus, since the numerical results in Sect. 5.1 show amplification for the case without these simplifying assumptions, the effects of e.g. ionization and a temperature gradient tend to work together with the radiative force and its derivatives to overcome the damping contribution from the density gradient.

6. Conclusions and speculations

It has been shown that H-deficient model atmospheres may have radiative forces which exceed gravity, similar to the case of some luminous H-rich stars (Lamers & Fitzpatrick 1988; Gustafsson & Plez 1992). Such super-Eddington luminosities manifest themselves as P_{gas} -inversions in hydrostatic atmospheres. The inversions are, however, not an artifact of this assumption but can also be present in dynamical atmospheres. The inversions are not removed unless a very high mass loss rate is present, and is neither necessarily removed by convection if the large radiative forces occur close to the surface. Thus, super-Eddington luminosities does *not* automatically initiate a stellar wind.

The location of the H-deficient R CrB stars in the immediate proximity of the computed opacity-modified Eddington limit (Fig. 2), is certainly suggestive of a connection between the enigmatic visual declines of the stars and the Eddington limit. It is therefore proposed that instabilities as the R CrB stars encounter the Eddington limit during their evolution towards higher T_{eff} are the unknown trigger mechanism for their famous variability. The Eddington limit may thus be the “smoking gun” for the declines: gas is ejected due to the high radiative forces in the atmospheres, which then cools rapidly first radiatively and later from adiabatic expansion to reach sub-equilibrium temperatures and thus possibly enable dust condensation (cf. Woitke et al. 1996 for the similar case of shocks instead induced by pulsations). Such gas ejections may be observable as absorption components in strong lines, as observed by Rao & Lambert (1997) in R CrB at maximum light. If a connection indeed exists, it could explain why the EHe and HdC stars do not show R CrB-like variability as a result of being located on the stable side of the Eddington limit. It also points to an interesting similarity between the R CrB stars and the LBVs. Thus, the two types of stars known to be situated at the Eddington limit both show eruptive behaviour, which suggests a similar underlying physical explanation for their variability.

A search for radiative and dynamical instabilities in the atmospheres has been carried out for both H-rich and H-deficient late-type supergiants, but only partly successfully. Sound waves are found to be amplified by the large radiative forces but the linear stability analysis reveal only rather slow growth rates compared to for early-type stars despite the super-Eddington luminosities. Such radiation-modified sound waves may thus be partly responsible for the semi-regular pulsational variations of such supergiants, but it is doubtful whether the instability is efficient enough to eject gas clouds from the atmospheres as

speculated above. The atmospheres are also found to be close to dynamically unstable, which might give rise to increased mass loss, as previously suggested for LBVs (Stothers & Chin 1993) and for the termination of the AGB phase (e.g. Paczyński & Ziółkowski 1968; Wagenhuber & Weiss 1994). This does not, however, explain in what way the R CrB stars are special compared to other similar stars. In fact, the H-rich models seem to be more vulnerable to such instabilities, which suggests that dynamical instabilities are not the answer to the declines of the R CrB stars. Another possibility is of course that the same dynamical instabilities occur in both types of stars but that the H-deficient and C-rich environment of the R CrB stars greatly favours dust condensation, and thus the observational manifestation, compared to for H-rich compositions.

One can also imagine that the Eddington limit is still responsible for the behaviour of the R CrB stars though in a more indirect way. Langer (1997a,b) has shown that the effect of rotation coupled with strong radiative forces may lead to increased mass loss in the equatorial plane, and it is possible that such a mechanism is at work in these supergiants, despite the presumably relatively small rotational velocities. The difference in observed variability between the R CrB stars and the HdC and EHe stars could then be the result of viewing angle. There are some observational evidence for such bipolarity (e.g. Rao & Lambert 1993; Clayton et al. 1997). Violent instabilities due to strange mode pulsations leading to dramatically increased mass loss is another possibility, which is partly related to the Eddington limit, since both have their origin in ionization zones, as do the dynamical instabilities discussed above. Whether any of these instabilities, or a combination thereof, could help explain the variability of the R CrB stars and the LBVs certainly deserves further investigation.

Finally, it should be remembered that the stability analyses presented here assume the unperturbed model to be a realistic description of the stellar atmosphere. At least for the R CrB stars, there are strong indications that this is in fact not the case (Gustafsson & Asplund 1996; Asplund et al. 1997a,b,c; Lambert et al. 1997). If the supergiant atmospheres are indeed distinctly different from the predictions of standard models, the efficiency of radiative instabilities may have been underestimated. One can suspect that models based on the normal assumptions, such as the mixing length theory for convection, near the Eddington limit may be very unsuitable. Clearly, radiative hydrodynamical simulations of such atmospheres would be valuable, also since they would shed further light on possible instabilities.

Acknowledgements. The constructive suggestions by F.P. Pijpers and A. Weiss have significantly improved the paper. Discussions with W. Glatzel, B. Gustafsson, L.-A. Willson and P. Woitke have been very helpful. The author is grateful to L. Achmad, H.J.G.L.M. Lamers, N. Langer and S. Owocki for communicating their work prior to publication.

References

Achmad L., Lamers H.J.G.L.M., 1997, A&A 320, 196

- Asplund M., Gustafsson B., 1996, in: Hydrogen-deficient stars, Jeffery C.S., Heber U. (eds.). ASP conf. series 96, p. 39
- Asplund M., Gustafsson B., Kiselman D., Eriksson K., 1997a, A&A 318, 521
- Asplund M., Gustafsson B., Lambert D.L., Rao N.K., 1997b, A&A 321, L17
- Asplund M., Gustafsson B., Rao N.K., Lambert D.L., 1997c, A&A, in press
- Berthomieu G., Provost J., Rocca A., 1976, A&A 47, 413
- Carlberg R.G., 1980, ApJ 241, 1131
- Clayton G.C., 1996, PASP 108, 225
- Clayton G.C., Bjorkman K.S., Nordsieck K.H., Zellner N.E.B., Schulte-Ladbeck R.E., 1997, ApJ 476, 870
- Eddington A.S., 1926, The internal constitution of the stars, Cambridge University Press, Cambridge
- Feast M.W., 1986, in: Hydrogen-deficient stars and related objects, Hunger K., Schönberner D., Rao N.K. (eds.). Reidel, Dordrecht, p. 151
- Gustafsson B., Asplund M., 1996, in: Hydrogen-deficient stars, Jeffery C.S., Heber U. (eds.). ASP conf. series 96, p. 27
- Gustafsson B., Plez B., 1992, in: Instabilities in evolved super- and hypergiants, de Jager C., Nieuwenhuijzen H. (eds.). North Holland, Amsterdam, p. 86
- Hearn A.G., 1972, A&A 19, 417
- Hearn A.G., 1973, A&A 23, 97
- Humphreys R.M., Davidson K., 1994, PASP 106, 1025
- Jeffery C.S., 1996, in: Hydrogen-deficient stars, Jeffery C.S., Heber U. (eds.). ASP conf. series 96, p. 152
- Kilkenny D., 1982, MNRAS 200, 1019
- Lambert D.L., Rao N.K., Gustafsson B., Asplund M., 1997, A&A, in press
- Lamers H.J.G.L.M., Fitzpatrick E.L., 1988, ApJ 324, 279
- Langer N., 1997a, in: Luminous Blue Variables: massive stars in transition, Nota A., Lamers H.J.G.L.M. (eds.). ASP conf. series 120, p. 83
- Langer N., 1997b, A&A, in press
- Lawson W.A., Cottrell P.L., 1997, MNRAS 285, 266
- Lobel A., Achmad L., de Jager C., Nieuwenhuijzen H., 1992, A&A 264, 147
- Maeder A., 1989, in: Physics of luminous blue variables, Davidson K., Moffat A.F.J., Lamers H.J.G.L.M. (eds.). Kluwer, Dordrecht, p. 15
- Mihalas D., 1978, Stellar atmospheres, W.H. Freeman and Company, San Francisco
- Mihalas D., Weibel Mihalas B., 1984, Foundations of radiation hydrodynamics, Oxford University Press, Oxford
- Nieuwenhuijzen H., de Jager C., 1995, A&A 302, 811
- Owocki S.P., Gayley K.G., 1997, in: Luminous Blue Variables: massive stars in transition, Nota A., Lamers H.J.G.L.M. (eds.). ASP conf. series 120, p. 121
- Paczyński B., Ziółkowski J., 1968, Acta Astr. 18, 225
- Rao N.K., Lambert D.L., 1993, AJ 105, 1915
- Rao N.K., Lambert D.L., 1997, MNRAS 284, 489
- Seaton M.J., Yan Y., Mihalas D., Pradhan A.K., 1994, MNRAS 266, 805
- Spiegel E.A., 1976, in: Physique des mouvements dans les atmosphères stellaires, Cayrel R., Steinberg M. (eds), CNRS, Paris, p. 19
- Stothers R.B., Chin C.-w., 1993, ApJ 408, L85
- Wagenhuber J., Weiss A., 1994, A&A 290, 807
- Woitke P., Goeres A., Sedlmayr E., 1996, A&A 313, 217